Structural Engineering and Mechanics, *Vol. 54, No. 3 (2015) 433-451*
DOI: http://dx.doi.org/10.12989/sem.2015.54.3.433

Large deflection analysis of edge cracked simple supported beams

Şeref Doğuşcan Akbaş*

Department of Civil Engineering, Bursa Technical University,152 Evler Mah., Eğitim Cad., 1. Damla Sok., No: 2/10, 16330 Yıldırım, Bursa, Turkey

(Received January 1, 2014, Revised October 16, 2014, Accepted November 6, 2014)

Abstract. This paper focuses on large deflection static behavior of edge cracked simple supported beams subjected to a non-follower transversal point load at the midpoint of the beam by using the total Lagrangian Timoshenko beam element approximation. The cross section of the beam is circular. The cracked beam is modeled as an assembly of two sub-beams connected through a massless elastic rotational spring. It is known that large deflection problems are geometrically nonlinear problems. The considered highly non-linear problem is solved considering full geometric non-linearity by using incremental displacement-based finite element method in conjunction with Newton-Raphson iteration method. There is no restriction on the magnitudes of deflections and rotations in contradistinction to von-Karman strain displacement relations of the beam. The beams considered in numerical examples are made of Aluminum. In the study, the effects of the location of crack and the depth of the crack on the non-linear static response of the beam are investigated in detail. The relationships between deflections, end rotational angles, end constraint forces, deflection configuration, Cauchy stresses of the edge- cracked beams and load rising are illustrated in detail in non-linear case. Also, the difference between the geometrically linear and nonlinear analysis of edge-cracked beam is investigated in detail.

Keywords: open edge crack; total Lagrangian finite element model; circular beams; timoshenko beam; large displacements; large rotations

1. Introduction

In recent years, with the development of technology, increasing demands for optimum or minimum-weight designed structural components makes it necessary to use non-linear theory of beams. Especially, developments in aerospace engineering, robotics and manufacturing make it inevitable to excessively use non-linear models that must be solved numerically. Because, a closed-form solution is not possible and hence more general numerical processes play an important role.

Many optimum or minimum-weight designed structural components are under severe operational conditions. In many cases, the small deflection linear theory is no longer applicable. It is very necessary to use and understand crack and fracture behaviour with non-linear analysis.

*Corresponding author, Assistant Professor, E-mail: serefda@yahoo.com

http://www.techno-press.org/?journal=sem&subpage=8 ISSN: 1225-4568 (Print), 1598-6217 (Online)

Structural elements are subjected to destructive effects in the form of initial defects within the material or caused by fatigue or stress concentration. As a result of destructive effects, cracks occur in the structural elements. It is known that cracks cause local flexibility and changes in structural stiffness. Understanding the mechanical behavior edge-cracked structures and detection of cracks are very important for safety of structures. In the literature, investigation in the non-linear analysis of cracked beams is very limited. In the literature, studies of the nonlinear behavior of cracked beams are as follows; Post buckling behavior of a column with a transverse surface crack on the one side is studied by Anifantis and Dimarogonas (1984). Sundermeyer and Weaver (1995) used nonlinear vibration character of a cracked beam for determining crack location, depth and opening load. Chen *et al*. (2006) investigated the detection of newly induced damage in reinforced concrete beams by using transient characteristics of nonlinear vibration. Peng *et al*. (2008) analyzed nonlinear output frequency response functions for cracked beams. Mokashi and Mendelsohn (2008) examined quasistatic nonlinear moment-slope relation for an edge-cracked beam element with a strictly linear softening cohesive zone ahead of the crack tip. Mendelsohn *et al*. (2008) present nonlinear free vibration analysis of an Euler-Bernoulli beam with an edge and a cohesive zone at the crack tip by using bending and shear springs. Dutta *et al*. (2009) investigated a crack detection technique based on nonlinear acoustics. Kitipornchai *et al*. (2009) analyzed nonlinear vibration of beams made of functionally garded materials containing an open edge crack by using Timoshenko beam theory and von Karman geometric nonlinearity. Ke *et al*. (2009) used Ritz method to find solutions to the post-buckling behavior of FGM beams with an open edge crack based on Timoshenko beam theory and von Kármán nonlinear kinematics. Kocatürk and Akbaş (2010) examined geometrically nonlinear behavior of simple supported beams within 2-D solid continuum approximation. Douka *et al*. (2010) studied nonlinear vibration technique for fatigue crack detection in beam-like structures using frequency mixing. Banik (2011) presents nonlinear responses behavior of a cracked reinforced concrete beam under harmonic excitation. Chatterjee (2011) studied damage assessments of cantilever beams under harmonic excitation by using nonlinear vibration response. Akbaş (2013) investigated geometrically nonlinear static analysis of edge cracked Functionally graded Timoshenko beam by using Total Langragian finite element method. Yan *et al*. (2012) discussed the nonlinear flexural dynamic behavior of a clamped Timoshenko beam made of FGM with an open edge crack under an axial parametric excitation which is a combination of a static compressive force and a harmonic excitation force based on Timoshenko beam theory and von Kármán nonlinear kinematics. Andreasus and Baragatti (2012) imvestigated experimental damage detection of cracked steel beams by using nonlinear characteristics of flexural forced vibration response. Younesian *et al*. (2013) investigated the frequency response of a cracked beam supported by a nonlinear viscoelastic foundation. Giannini *et al*. (2013) analyzed the nonlinear dynamic behavior of structures with breathing cracks forced by harmonic excitation. Wei *et al*. (2013) discussed the nonlinear response characteristics of a cracked beam subjected to a high-frequency acoustic wave. Akbaş (2014a, b, c) studied wave propagation of edge cracked beams under impact loads.

It is seen from literature that that investigations of the full geometrically nonlinear analysis of edge cracked beams are very limited. It is seen from literature that the nonlinear studies of edge cracked beams are investigated within von Karman nonlinear strain approximation in which full geometric non-linearity cannot be considered. In von Karman nonlinear strain approximation, because of neglect of some components of strain, satisfactory results can be obtained only for large displacements but moderate rotations. It is known that large deflection problems are geometrically nonlinear problems. In the present study, the large deflection analysis of edge cracked beams is

considered by using the total Lagrangian finite element method by taking into account full geometric nonlinearity. There is no restriction on the magnitudes of deflections and rotations in contradistinction to von-Karman strain displacement relations of the beam.

In this study, large deflection static behavior of edge cracked simple supported circular beams subjected to a non-follower transversal point load at the midpoint of the beam is studied by using the total Lagrangian Timoshenko beam element approximation. The cracked beam is modeled as an assembly of two sub-beams connected through a massless elastic rotational spring. The considered highly non-linear problem is solved considering full geometric non-linearity by using incremental displacement-based finite element method in conjunction with Newton-Raphson iteration method. The distinctive feature of this study is large deflection static analysis of edge cracked circular beams considering full geometric non-linearity. Another distinctive feature of this study is investigation of the differences of the analysis results in the case of geometrically linear and geometrically nonlinear.

The development of the formulations of general solution procedure of nonlinear problems follows the general outline of the derivation given by Zienkiewicz and Taylor (2000). The related formulations of geometrically nonlinear static analysis of edge cracked Timoshenko beam subjected to a non-follower transversal point load at the midpoint of the beam are obtained by using the total Lagrangian finite element model. In deriving the formulations for geometrically nonlinear analysis of edge cracked Timoshenko beams, the total Lagrangian Timoshenko beam element formulations for given by Felippa (2013) are used. In the study, the effects of the location of crack and the depth of the crack on the non-linear static response of the beam are investigated in detail. The relationships between deflections, end rotational angles, end constraint forces, deflection configuration, Cauchy stresses of the edge- cracked beams and load rising are illustrated in detail in non-linear case. Also, the difference between the geometrically linear and nonlinear analysis of edge-cracked beam is investigated in detail.

2. Theory and formulations

A simple supported circular beam of length L, diameter D, containing an edge crack of depth a located at a distance from the left end L_1, as shown in Fig. 1. One of the supports of the beam is assumed to be pinned and the other is rolled. It is assumed that the crack is perpendicular to beam surface and always remains open. The beam is subjected to a non-follower transversal point load (P) at the midpoint of the beam in the transverse direction as seen from Fig. 1.

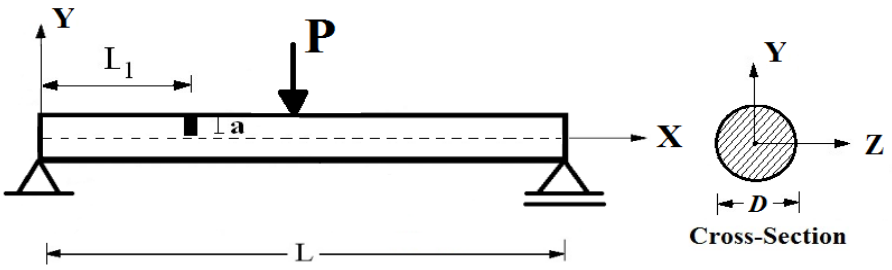

Fig. 1 A simple supported circular beam with an open edge crack subjected to a non-follower point load at the midpoint of the beam and cross-section

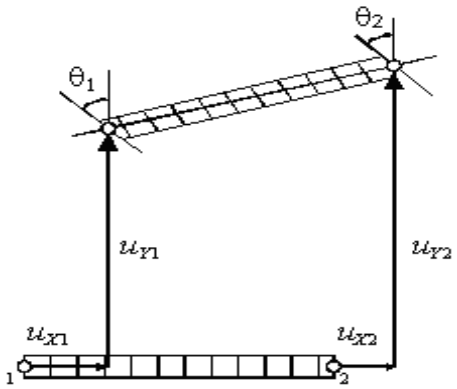

Fig. 2 A two-node C^0 beam element

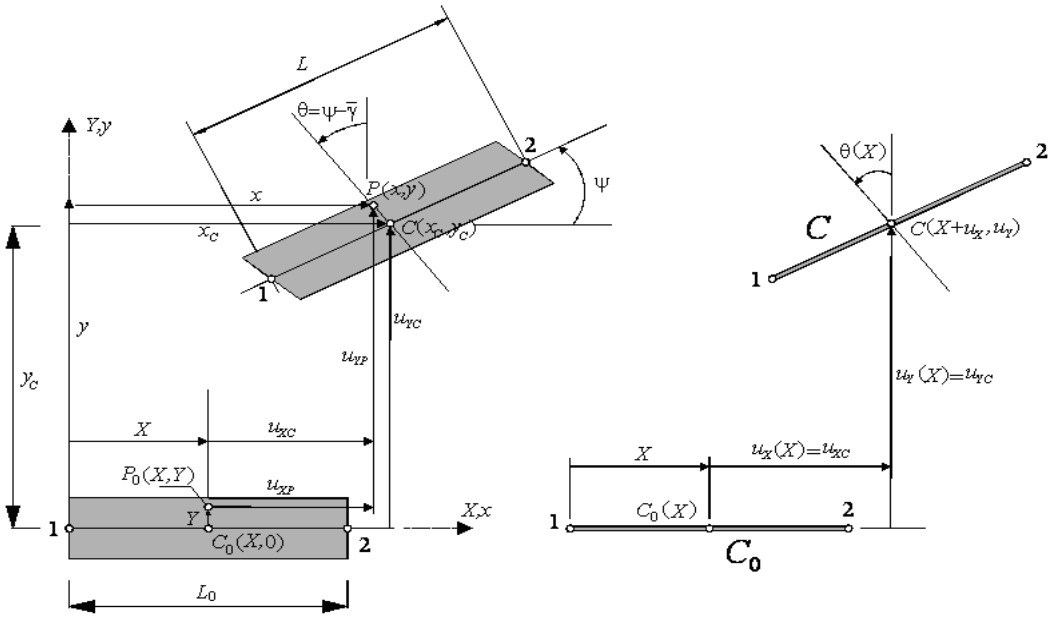

(a) (b)

Fig. 3 Lagrangian kinematics of the C^0 beam element with X-aligned reference configuration: (a) plane beam moving as a two-dimensional body; (b) reduction of motion description to one dimension measured by coordinate X. This figure is given by Felippa (2013)

2.1 Total Lagrangian finite element formulations of intact Timoshenko beams

In this study, the Total Langragian Timoshenko beam element is used and the related formulations are developed by using the formulations given by Felippa (2013). In the present study, finite element model of Timoshenko beam element is developed by using a two-node beam element shown in Fig. 2. Each node has three degrees of freedom: Two node displacements u_{xi} and u_{yi}, and one rotation θ_i about Z axis.

A particle originally located at $P_0(X, Y)$ moves to $P(x, y)$ in the current configuration, as shown in Fig. 3. The projections of P_0 and P along the cross sections at C_0 and C upon the neutral axis are called $C_0(X, 0)$ and $C(x_c, y_c)$, respectively. It will be assumed that dimensions of the beam cross section do not change, and that the shear distortion $\gamma<<1$ so that $\cos\gamma$ can be replaced by 1 (Felippa 2013).

$$x = x_c - Y(\sin\psi + \sin\gamma\cos\psi) = x_c - Y[\sin(\psi+\gamma) + (1-\cos\gamma)\sin\psi] = x_c - Y\sin\theta \tag{1}$$

$$y = y_c + Y(\cos\psi - \sin\gamma\sin\psi) = y_c + Y[\sin(\psi+\gamma) + (1-\cos\gamma)\cos\psi] = y_c + Y\cos\theta \tag{2}$$

where $x_c=X+u_{XC}$ and $y_c=u_{XC}$. Consequently, $x=X+u_{XC}-Y\sin\theta$ and $y=u_{YC}+Y\cos\theta$. From now on we shall call u_{XC} and u_{YC} simply u_X and u_Y, respectively, so that the Lagrangian representation of the motion is

$$\begin{bmatrix} x \\ y \end{bmatrix} = \begin{bmatrix} X + u_X - Y\sin\theta \\ u_Y + Y\cos\theta \end{bmatrix} \tag{3}$$

in which u_X, u_Y and θ are functions of X only. This concludes the reduction to a one-dimensional model, as sketched in Fig. 3(b). For a two-node C_0 element, it is natural to express the displacements and rotation functions as linear in between the node displacements:

$$\mathbf{w} = \begin{bmatrix} u_X(X) \\ u_Y(X) \\ \theta(X) \end{bmatrix} = \frac{1}{2}\begin{bmatrix} 1-\xi & 0 & 0 & 1+\xi & 0 & 0 \\ 0 & 1-\xi & 0 & 0 & 1+\xi & 0 \\ 0 & 0 & 1-\xi & 0 & 0 & 1+\xi \end{bmatrix} \begin{bmatrix} u_{X1} \\ u_{Y1} \\ \theta_1 \\ u_{X2} \\ u_{Y2} \\ \theta_1 \end{bmatrix} = \mathbf{Nu} \tag{4}$$

in which $\xi=(2X/L_0)-1$ is the isoparametric coordinate that varies from $\xi=-1$ at node 1 to $\xi=1$ at node 2.

The Green-Lagrange strains are given as follows Felippa (2013)

$$[e] = \begin{bmatrix} e_1 \\ e_2 \end{bmatrix} = \begin{bmatrix} e_{XX} \\ 2e_{XY} \end{bmatrix} = \begin{bmatrix} (1+u'_X)\cos\theta + u'_Y\sin\theta - Y\theta' - 1 \\ -(1+u'_X)\sin\theta + u'_Y\sin\theta \end{bmatrix} = \begin{bmatrix} e - Y\kappa \\ \gamma \end{bmatrix} \tag{5}$$

$$e = (1+u'_X)\cos\theta + u'_Y\sin\theta - 1; \quad \gamma = -(1+u'_X)\sin\theta + u'_Y\sin\theta; \quad \kappa = \theta' \tag{6}$$

where e is the axial strain, γ is the shear strain and κ is curvature of the beam, $u'_x = du_X/dX$, $u'_Y = du_Y/dX$, $\theta'=d\theta/dX$.

According to Hooke's law, constitutive equations of the beam with the second Piola-Kirchhoff stresses are as follows

$$\mathbf{S} = \begin{bmatrix} S_{XX} \\ S_{XY} \end{bmatrix} = \begin{bmatrix} s_1 \\ s_2 \end{bmatrix} = \begin{bmatrix} s_1^0 + Ee_1 \\ s_2^0 + Ge_2 \end{bmatrix} \tag{7}$$

where s_1^0, s_2^0 are initial stresses, E is the modulus of elasticity, G is the shear modulus. Using constitutive equations, axial force N, shear force V and bending moment M can be obtained as

$$N = \int_A s_1 \, dA = \int_A [s_1^0 + Ee_1] dA = N^0 + Ee_1 A \tag{8}$$

$$V = \int_A s_2 \, dA = \int_A [s_2^0 + Ge_2] dA = V^0 + GA\gamma \tag{9}$$

$$M = \int_A -Ys_1 \, dA = \int_A -Y[s_1^0 + Ee_1] dA = M^0 + EI_0\kappa \tag{10}$$

where

$$N^0 = \int_{A_0} s_1^0 dA, \quad V^0 = \int_{A_0} s_2^0 dA, \quad M^0 = \int_{A_0} -Ys_1^0 dA \tag{11}$$

For the solution of the total Lagrangian formulations of Timoshenko beam problem, small-step incremental approaches from known solutions are used. As it is known, it is possible to obtain solutions in a single increment of the external force only in the case of mild nonlinearity (and no path dependence). To obtain realistic answers, physical insight into the nature of the problem and, usually, small-step incremental approaches from known solutions are essential. Such incremental procedures are useful to reduce excessive numbers of iterations and in following the physically correct path. In the iterations, the load is divided by a suitable number according to the value of load. The loading is divided by large numbers. After completing an iteration process, the load is increased by adding load increment to the accumulated load.

In this study, small-step incremental approaches from known solutions with Newton-Raphson iteration method are used in which the solution for n+1 th load increment and i th iteration is obtained in the following form

$$d\,\mathbf{u}_n^i = (\mathbf{K}_T^i)^{-1} \mathbf{R}_{n+1}^i \tag{12}$$

where (K_T^i) is the system stiffness matrix corresponding to a tangent direction at the i th iteration, $d\,\mathbf{u}_n^i$ is the solution increment vector at the i th iteration and n+1 th load increment, $(R_{n+1}^i)_S$ is the system residual vector at the i th iteration and n+1 th load increment. This iteration procedure is continued until the difference between two successive solution vectors is less than a selected tolerance criterion in Euclidean norm given by

$$\sqrt{\frac{[(d\mathbf{u}_n^{i+1} - d\mathbf{u}_n^i)^T (d\mathbf{u}_n^{i+1} - d\mathbf{u}_n^i)]^2}{[(d\mathbf{u}_n^{i+1})^T (d\mathbf{u}_n^{i+1})]^2}} \le \varsigma_{tol} \tag{13}$$

A series of successive approximations gives

$$\mathbf{u}_{n+1}^{i+1} = \mathbf{u}_{n+1}^i + d\mathbf{u}_{n+1}^i = \mathbf{u}_n + \Delta\mathbf{u}_n^i \tag{14}$$

where

$$\Delta\mathbf{u}_n^i = \sum_{k=1}^{i} d\mathbf{u}_n^k \tag{15}$$

The residual vector R_{n+1}^i for a finite element is as follows

$$\mathbf{R}_{n+1}^{i} = \mathbf{f} - \mathbf{p} \tag{16}$$

where **f** is the vector of external forces and **p** is the vector of internal forces given in Appendix.

The element tangent stiffness matrix for the total Lagrangian Timoshenko plane beam element is as follows which is given by Felippa (2013)

$$\mathbf{K}_T = \mathbf{K}_M + \mathbf{K}_G \tag{17}$$

where $\mathbf{K}_G$ is the geometric stiffness matrix, and $\mathbf{K}_M$ is the material stiffness matrix given as follows by Felippa (2013)

$$\mathbf{K}_M = \int_{L_0} \mathbf{B}_m^T \mathbf{S} \mathbf{B}_m dX \tag{18}$$

The explicit forms of the expressions in Eq. (17) is given in Appendix. After integration of Eq. (18), K_M can be expressed as follows

$$\mathbf{K}_M = \mathbf{K}_M^a + \mathbf{K}_M^b + \mathbf{K}_M^s \tag{19}$$

where $\mathbf{K}_M^a$ is the axial stiffness matrix, $\mathbf{K}_M^b$ is the bending stiffness matrix, $\mathbf{K}_M^s$ is the shearing stiffness matrix and explicit forms of these expressions are given in Appendix. The geometric stiffness matrix K_G, $\mathbf{B}_m$ and the internal nodal force vector **p** remain given in Appendix.

2.2 Crack modeling

The cracked beam is modeled as an assembly of two sub-beams connected through a massless elastic rotational spring shown in Fig. 4.

The bending stiffness of the cracked section k_T is related to the flexibility G by

$$k_T = \frac{1}{G} \tag{20}$$

Cracked section's flexibility G can be derived from Broek's approximation (Broek 1986)

$$\frac{(1-\upsilon^2)K_I^2}{E} = \frac{M^2}{2}\frac{dG}{da} \tag{21}$$

where M is the bending moment at the cracked section, K_I is the stress intensity factor (SIF) under mode I bending load and is a function of the geometry and the loading properties as well. υ indicates Poisson's ratio. For circular cross section, the stress intensity factor for K_I a single edge cracked beam specimen under pure bending M can be written as follow (Tada *et al*. 1985)

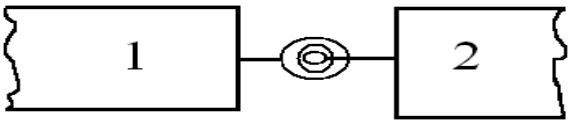

Fig. 4 Rotational spring model

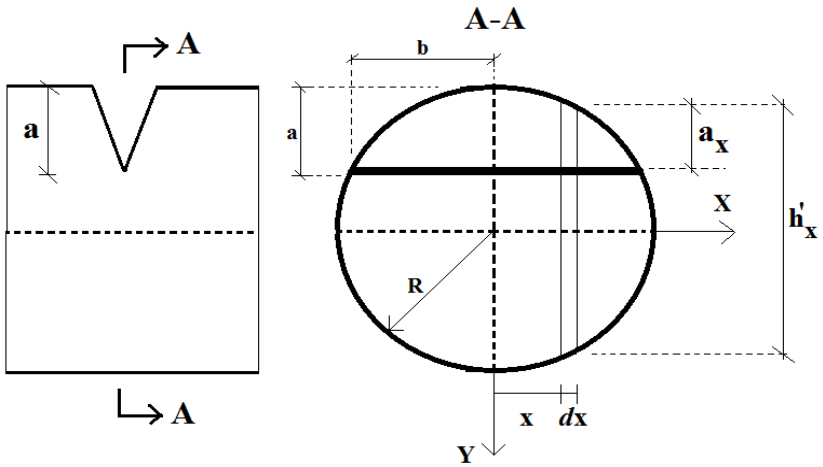

Fig. 5 The geometry of the cracked circular cross section

$$K_I = \frac{4M}{\pi R^4}\frac{h'_x}{2}\sqrt{\pi a}F(a/h'_x) \tag{22}$$

Where

$$F(a/h'_x) = \sqrt{\frac{2h'_x}{\pi a}tg(\frac{\pi a}{2h'_x})}\frac{0.923+0.199(1-\sin(\frac{\pi a}{2h'_x}))^4}{\cos(\frac{\pi a}{2h'_x})} \tag{23}$$

Where a is crack of depth and h'_x is the height of the strip, is shown Fig. 5, and written as

$$h'_x = 2\sqrt{R^2 - x^2} \tag{24}$$

where R is the radius of the cross section of the beam.

After substituting Eq. (22) into Eq. (21) and by integrating Eq. (21), the flexibility coefficient of the crack section G is obtained as

$$G = \frac{32(1-\upsilon^2)}{E\pi R^8}\int_{-b}^{b}\int_{0}^{a_x} y(R^2-x^2)F^2(a/h'_x)dy\,dx \tag{25}$$

where b and a_x are the boundary of the strip and the local crack depth respectively, are shown in Fig. 5, respectively, and written as

$$b = \sqrt{R^2-(R-a)^2} \tag{26}$$

$$a_x = \sqrt{R^2 = x^2} - (R-a) \tag{27}$$

The spring connects the adjacent left and right elements and couples the slopes of the two beam elements at the crack location. In the massless spring model, the compatibility conditions enforce

the continuities of the axial displacement, transverse deflection, axial force and bending moment across the crack at the cracked section ($X=L_1$), that is

$$\mathrm{v}_1 = \mathrm{v}_2 , \quad \mathrm{M}_1 = \mathrm{M}_2 \tag{28}$$

The discontinuity in the slope is as follows

$$k_T(\frac{dv_1}{dX} - \frac{dv_2}{dX}) = k_T(\theta_1 - \theta_2) = M_1 \tag{29}$$

Based on the massless spring model, the stiffness matrix of the cracked section as follows

$$[K]_{(Cr)} = \begin{bmatrix} 1/G & -1/G \\ -1/G & 1/G \end{bmatrix} = \begin{bmatrix} k_r & -k_r \\ -k_r & k_r \end{bmatrix} \tag{30}$$

The stiffness matrix of the cracked section is written according to the displacement vector

$$\{q\}_{(cr)} = \{\theta_1, \theta_2\}^T \tag{31}$$

Where θ_1 and θ_2 are the angles of the cracked section. Addition with the crack model and by use of usual assemblage procedure, the system stiffness matrix is as follows

$$[K]_{(s)} = [K]_{(r)} + [K]_{(cr)} \tag{32}$$

Where $[K]_{(T)}$ is tangent stiffness matrix for the intact Timoshenko beam which is given Eq.(17).

After obtaining the displacements of nodes, the second Piola-Kirchhoff stress tensor components S_{xx}, S_{xy}, S_{yy} can be obtained by using Eq. (7). It is known that the relation between the Cauchy stress tensor components σ_{xx}, σ_{xy}, σ_{yy} and the second Piola-Kirchhoff stress tensor components S_{xx}, S_{xy}, S_{yy} can be written as follows

$$\sigma_{xx} = \frac{^2\rho}{^0\rho}\left(\frac{\partial x}{\partial X}\frac{\partial x}{\partial X}S_{xx} + 2\frac{\partial x}{\partial X}\frac{\partial x}{\partial Y}S_{xy} + \frac{\partial x}{\partial X}\frac{\partial x}{\partial Y}S_{yy}\right) \tag{33a}$$

$$\sigma_{yy} = \frac{^2\rho}{^0\rho}\left(\frac{\partial y}{\partial X}\frac{\partial y}{\partial X}S_{xx} + 2\frac{\partial y}{\partial X}\frac{\partial y}{\partial Y}S_{xy} + \frac{\partial y}{\partial Y}\frac{\partial y}{\partial Y}S_{yy}\right) \tag{33b}$$

$$\sigma_{xy} = \frac{^2\rho}{^0\rho}\left(\frac{\partial x}{\partial X}\frac{\partial x}{\partial X}S_{xx} + 2\frac{\partial x}{\partial X}\frac{\partial y}{\partial Y}S_{xy} + \frac{\partial x}{\partial Y}\frac{\partial x}{\partial Y}S_{yy}\right) \tag{33c}$$

where $^0\rho$ and ρ represent the mass densities of the material in configurations C_0 and C, respectively. The relations between the Lagrange coordinates X, Y and Euler coordinates x, y are given by Eqs. (1), (2). The relation between $^0\rho$ and ρ is as follows;

The relation between $^0\rho$ and ρ is as follows

$$^0\rho = \rho J \tag{34}$$

where J is the determinant of the deformation gradient tensor **F** (or the Jacobian of the transformation) and defined as follows

$$J = \det(F) = \begin{vmatrix} \frac{\partial x}{\partial X} & \frac{\partial x}{\partial Y} & \frac{\partial x}{\partial Z} \\ \frac{\partial y}{\partial X} & \frac{\partial y}{\partial Y} & \frac{\partial y}{\partial Z} \\ \frac{\partial z}{\partial X} & \frac{\partial z}{\partial Y} & \frac{\partial z}{\partial Z} \end{vmatrix} \tag{35}$$

In this study, it is assumed that ${}^{0}\rho$ and ρ.

3. Numerical results

In the numerical examples, the linear and the non-linear static displacements, end rotational angles, end constraint forces, deflection configuration, Cauchy stresses (true stresses) of the beams are calculated and presented in figures for different crack locations, crack depths. To this end, by use of usual assembly process, the system tangent stiffness matrix and the system residual vector are obtained by using the element stiffness matrixes and element residual vectors for the total Lagrangian Timoshenko plane beam element. After that, the solution process outlined in the previous section is used for obtaining the related solutions for the total Lagrangian finite element model of Timoshenko plane beam element. The beams considered in numerical examples are made of lower-carbon Aluminum: E=70 GPa v=0.33. In the numerical integrations, five-point Gauss integration rule is used. In the numerical calculations, the number of finite elements is taken as n=100. Unless otherwise stated, it is assumed that the diameter of the beam is D=0.2 m and length of the beam is L=3 m in the numerical results. In the geometrically non-linear case, the Cauchy stresses can be obtained by using Eqs. (33a-c) after obtaining the second Piola-Kirchhoff stresses by using equation (7).

In Figs. 6, 7 and 8, the vertical displacements of the midpoint *v(L/2)*, the left-end rotational

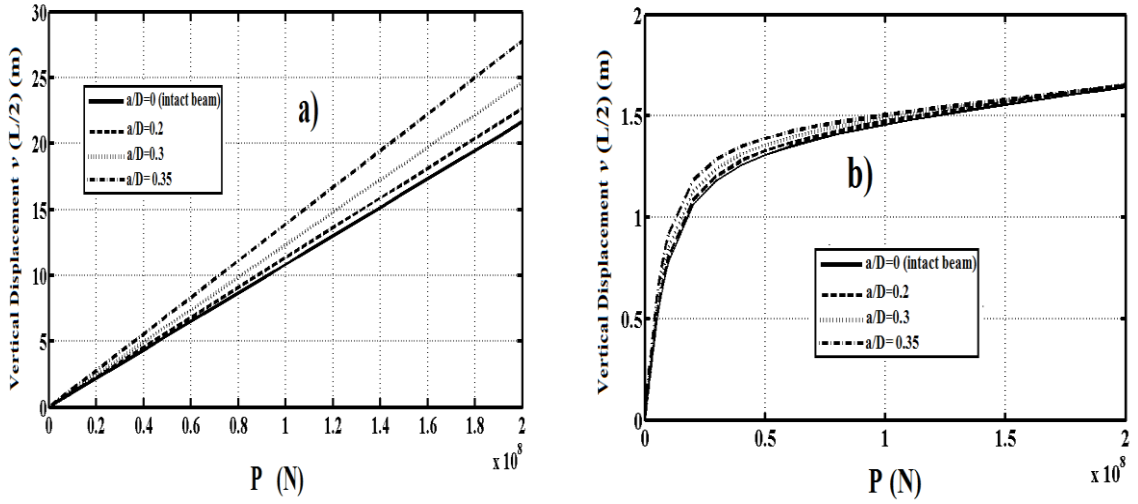

Fig. 6 Load-vertical displacements of the midpoint *v(L/2)* curves for different the crack depth ratios *a/D*, (a) linear case (b) non-linear case

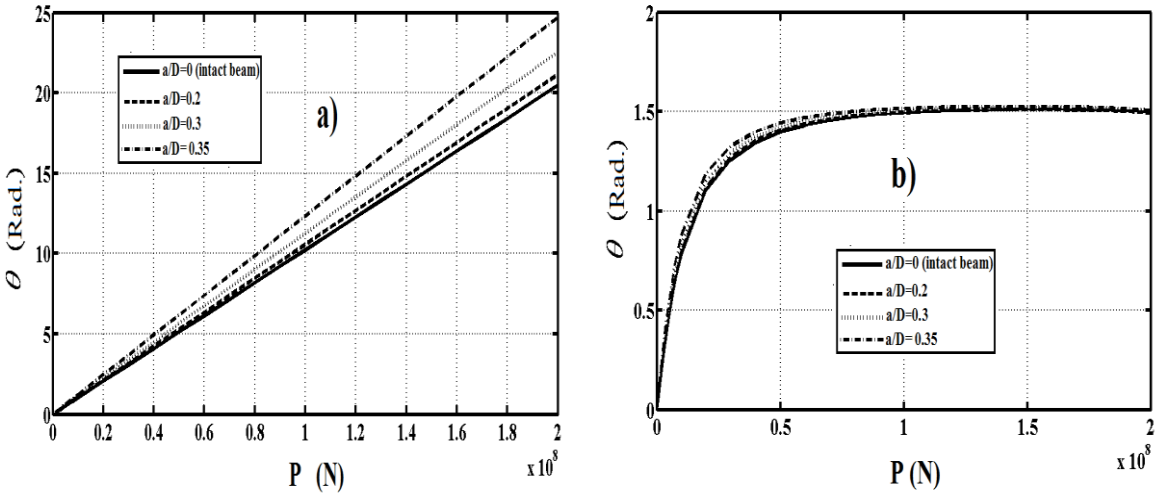

Fig. 7 Load-the left end rotational angle θ curves for different the crack depth ratios *a/D*, (a) Linear case (b) Non-linear case

angle θ (rad.) and the end constraint force R_V in the vertical direction versus load rising are presented , respectively, with different the crack depth ratios (*a/D*) for linear and nonlinear case for the crack location L_1/L=0.5.

It is seen from Figs. 6 and 7 that, with the increase in the crack depth (*a*/*D*), the displacements and rotaions increase, as expected. This is because by increasing the crack depth ratio (*a*/*D*), the beam becomes flexible. With the increase in the load, the effects of the crack on the beam increase significantly. Also, it is seen from Figs. 6 and 7 that there is a significant difference between the geometrically linear case and nonlinear case for the edge cracked beam. The increase in load causes increase in difference between the displacement values of the linear and the nonlinear solutions. Increase in load is more effective in the vertical displacements and rotations of the linear solution. Also, the difference between intact and cracked beam in the linear case is bigger than in the nonlinear's. This situation may be explained as follows: In the linear case, arm of the external forces or arm of the external resultant force do not change with the magnitude of the external forces, and therefore the displacements depend on the external forces linearly. However, in the case of nonlinear analysis, the arm of the external forces change with the magnitude of the external force and, as the magnitude of the force increases the arm of these external forces decrease. However, as the forces increase the configuration of the beam become close to vertical direction and therefore increase in the load does not cause a significant increase in displacements after certain load level in which the configuration of the beam is close to the vertical direction. Hence, the difference between intact and cracked beam in the linear case is bigger than the difference between intact and cracked beam in the nonlinear case.

It is seen from figure 8 that, with increase in the crack depth ratio, the end constraint forces R_V do not change in the linear case because the arm of the external forces or arm of the external resultant force do not change with the crack depth since. Whereas, with increase in the crack depth ratio, the end constraint forces R_V change in the nonlinear case because the arm of the external forces or arm of the external resultant force change with the crack depth.

In Fig. 9, the vertical displacements of the midpoint $v(L/2)$ versus load rising are presented with

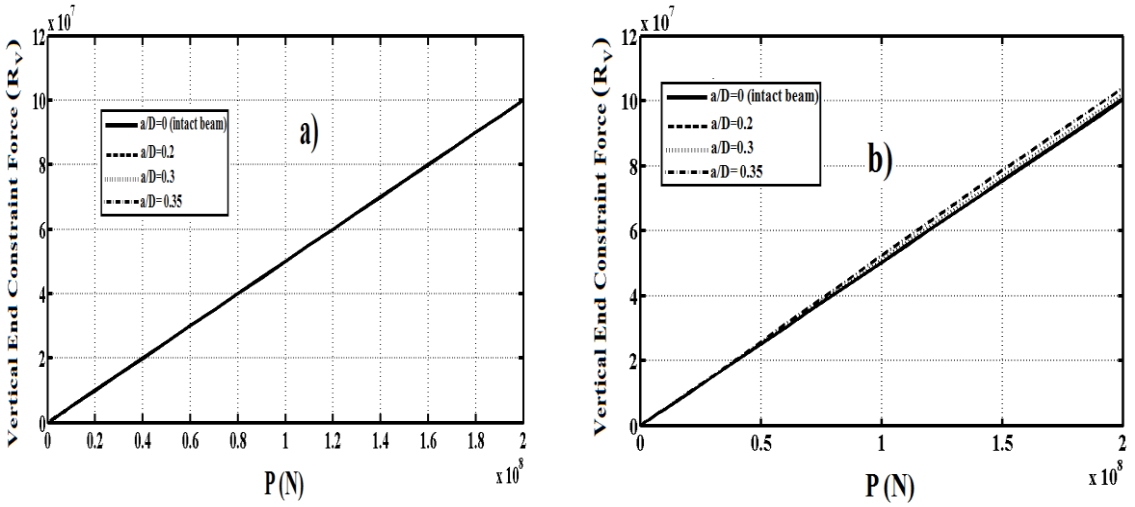

Fig. 8 Load-the end constraint force R_V curves for different the crack depth ratios *a/D*, (a) Linear case (b) Non-linear case

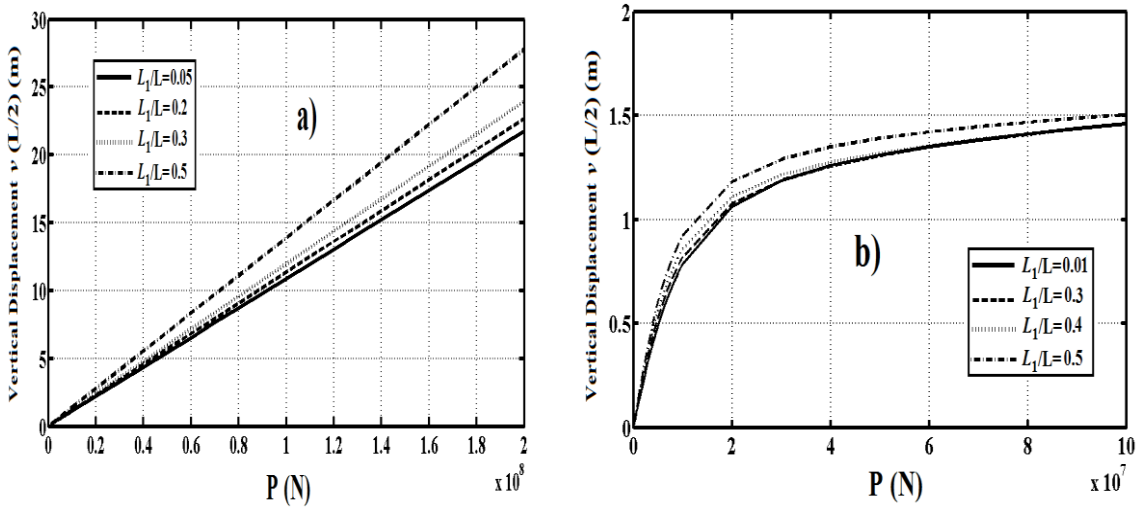

Fig. 9 Load-vertical displacements of the midpoint $v(L/2)$ curves for different the crack locations (L_1/L) from the left end, (a) Linear case (b) Non-linear case

different the crack locations (L_1/L) from the left end for linear and nonlinear case for the crack depth ratios a/D=0.35.

It is seen from Fig. 9 that, when the crack locations get closer to the midpoint of the beam, the displacements increase. This is because the crack at the midpoint of the beam has a most severe effect in the beam. It is observed from the Fig. 9 that there are significant differences of the analysis results for the linear case and nonlinear case.

Fig. 10 displays the effect of crack depth ratio (*a/D)* on the deflected shape of the beam for the crack location ratio L_1/L=0.5 from the left end and the point load is P=50000 kN for the geometrically linear and the nonlinear case.

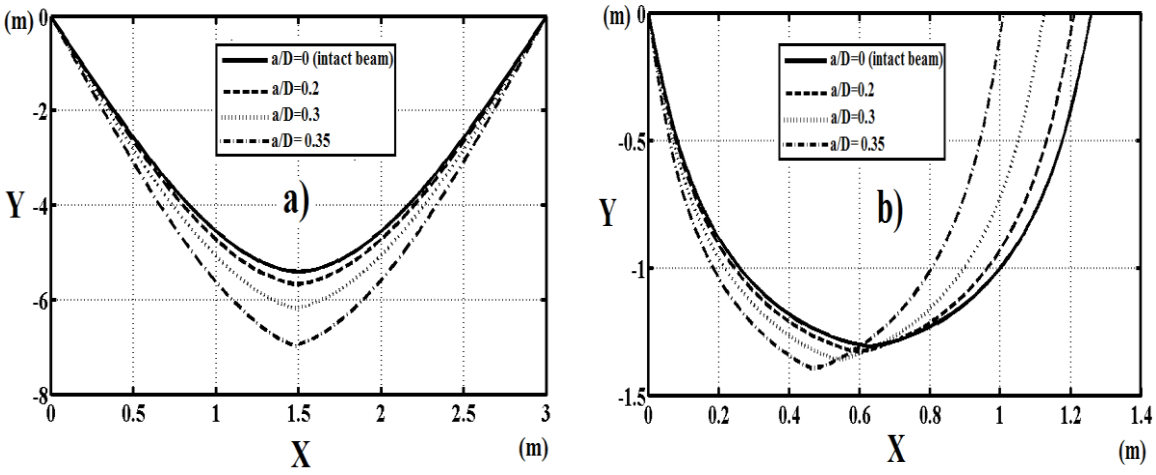

Fig. 10 The effect of the crack depth ratios (*a/D)* on the deflected shape of the beam for (a) Linear case (b) Non-linear case

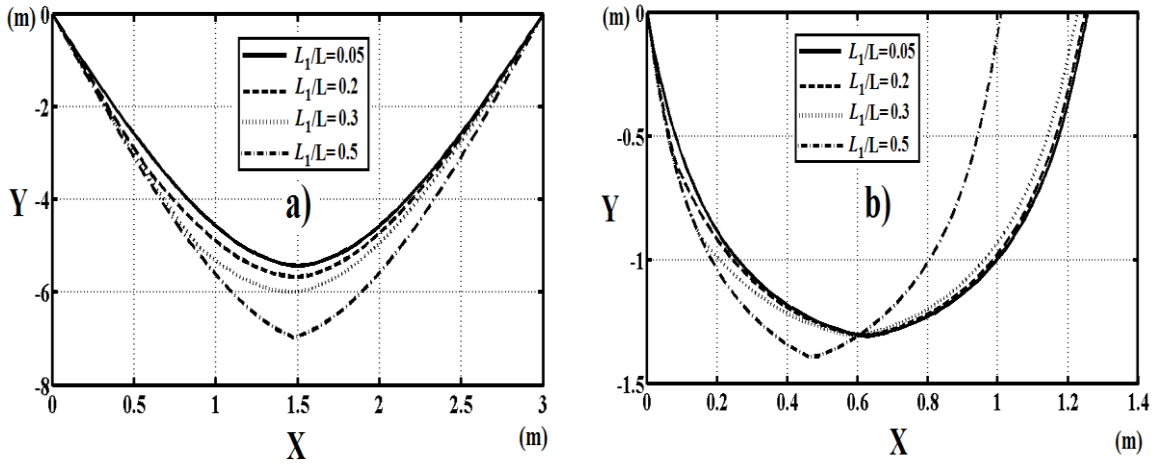

Fig. 11 The effect of the crack locations ratio (L_1/L) on the deflected shape of the beam for (a) Linear case (b) Non-linear case

In Fig. 11, the effect of crack locations ratio (L_1/L) on the deflected shape of the beam is presented for the crack depth ratio a/D=0.35 and the point load is P=50000 kN for the geometrically linear and the nonlinear case.

It is observed from figure 10 and 11 that he crack depth ratio (*a/D)* and the crack location ratio (L_1/L) play important role on the static response of the beam. There is a significant difference between the deformed configurations of the beam for linear case and nonlinear case. It shows that to learn about more realistic mechanical behaviour of the cracked beams, the geometrically nonlinear analysis must be considered.

In Fig. 12, Cauchy normal stresses in the X direction (σ_{xx}) at midpoint of the beam (X=1,5 m and Y=−0.1 m) versus load rising are presented with different the crack depth ratios (a/D) for the geometrically linear and the nonlinear case.

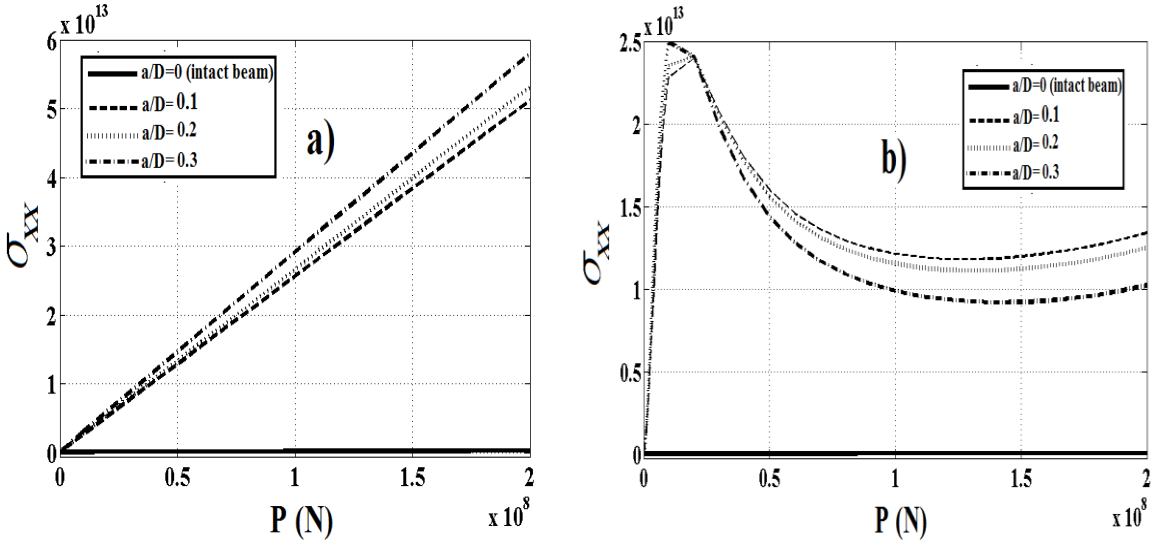

Fig. 12 The effect of the crack depth ratios (*a/D)* on the Cauchy normal stresses for (a) Linear case (b) Non-linear case

Fig. 12 shows that the crack depth is very effective in Cauchy stresses. With increase in the crack depth, Cauchy stresses increase seriously. It is seen Fig. 12 that stresses in the intact case are very small relative to crack case. This is because, when it has occurred a crack in the beam, the intensity of a stress field increase. As a result, high local stresses occur and the stresses can cause structures to fail more quickly. Also it is seen from Fig. 12, with increase in load, the difference between the linear case and nonlinear case increases for Cauchy normal stresses. It is observed from Fig. 12 that in the design and modeling of the structural elements in the crack must be considered with nonlinear analysis. The effect of the crack must be considered in the safe design of the structural elements because it can be occurred cracks in the structural elements after the construction.

4. Conclusions

Large deflection static analysis of edge cracked simple supported circular beams subjected to a non-follower transversal point load at the midpoint of the beam is studied by using the total Lagrangian Timoshenko beam element approximation. The cracked beam is modeled as an assembly of two sub-beams connected through a massless elastic rotational spring. The considered non-linear problem is solved by using incremental displacement-based finite element method in conjunction with Newton-Raphson iteration method. the effects of the location of crack and the depth of the crack on the non-linear static response of the beam are investigated in detail. It is observed from the results that the crack locations and the crack depth have a great influence on the geometrically non-linear behaviour of the beam. Also, it is seen from results that there are significant differences of the analysis results for the linear case and nonlinear case. Hence, the geometrically nonlinear case must be taken into account for safe design of edge cracked beams and for obtaining more realistic results. Otherwise an important error is inevitable. The effect of the

crack on the beams must be considered at the design stage because it can be occurred cracks in the structural elements after the construction. Future work should be devoted to the interpretation of the results in order to possible experimental investigation to validate the numerical results. Also, it would be interesting to demonstrate the ability of the procedure through a wider campaign of investigations concerning multi-cracked beams with different boundary conditions.

Acknowledgments

This work has been supported by Research Fund of the Bursa Technical University. Project Number: 2015-01-001.

References

Akbaş, Ş.D. (2013), "Geometrically nonlinear static analysis of edge cracked Timoshenko beams composed of functionally graded material", *Math. Prob. Eng.*, Article ID 871815, 14.

Akbaş, Ş.D. (2014a), "Wave propagation analysis of edge cracked circular beams under impact force", *Plos. One*, **9**(6), e100496.

Akbaş, Ş.D. (2014b), "Wave propagation analysis of edge cracked beams resting on elastic foundation", *Int. J. Eng. Appl. Sci*., **6**(1), 40-52.

Akbaş, Ş.D. (2014c), "Wave propagation in edge cracked functionally graded beams under impact force", *J. Vib. Control*, Doi: 10.1177/1077546314547531.

Andreasus, U. and Baragatti, P. (2012), "Experimental damage detection of cracked beams by using nonlinear characteristics of forced response", *Mech. Syst. Signal Pr.*, **31**, 382-404.

Anifantis, N. and Dimarogonas, A. (1984), "Post buckling behavior of transverse cracked columns", *Comput. Struct.*, **18**(2), 351-356.

Banik, A.K. (2011), "Nonlinear dynamics of cracked RC beams under harmonic excitation", *World Acad. Sci. Eng. Tech.*, **75**, 144-149.

Broek, D. (1986), *Elementary engineering fracture mechanics*, Martinus Nijhoff Publishers, Dordrecht.

Chartterjee, A. (2011), "Nonlinear dynamics and damage assessment of a cantilever beam with breathing edge crack", *J. Vib. Acoust. Trans. ASME*, **133**(5), 051004.

Chen, G., Yang, X., Ying, X. and Nanni, A. (2006), "Damage detection of concrete beams using nonlinear features of forced vibration", *Struct. Hlth. Monit.*, **5**(2), 125-141.

Douka, E., Zacharias, K.A., Hadjileıntiadis, L.J. and Trochidis, A. (2010), "Non-linear vibration technique for carck detection in beam structures using frequency mixing", *Acta Acustica Unites With Acustica*, **96**(5), 977-980.

Dutta, D., Sohn, H., Harries, K.A. and Rizzo, P. (2009), "A nonlinear acoustic technique for crack detection in metallic structures", *Struct. Hlth. Monit.*, **8**(3), 251-262.

Felippa, C.A. (2013), Notes on nonlinear finite element methods, http://www.colorado.edu/engineering/cas/courses.d/NFEM.d/NFEM.Ch10.d/NFEM.Ch10.pdf, Retrieved December 2013.

Giannini, O., Casini, P. and Vestroni, F. (2013), "Nonlinear harmonic identification of breathing cracks in beams", *Comput. Struct.*, **129**, 166-177.

Ke, L.L., Yang, J. and Kitipornchai, S. (2009), "Postbuckling analysis of edge cracked functionally graded Timoshenko beams under end shortening", *Compos. Struct.*, **90**(2), 152-160.

Kitipornchai, S., Ke, L.L., Yang, J. and Xiang, Y. (2009), "Nonlinear vibration edge cracked functionally graded Timoshenko beams", *J. Sound Vib.*, **324**(3-5), 962-982.

Kocaturk, T. and Akbaş, Ş.D. (2010), "Geometrically non-linear static analysis of a simply supported beam

made of hyperelastic material", *Struct. Eng. Mech.*, **35**(6), 677-697.
Mendelsohn, D.A., Vedacalam, S., Pecorari, C. and Mokasji, P.S. (2008), "Nonlinear vibration of an edge-cracked beam with a cohesive zone, 2: Perturbation analysis of Euler-Bernoulli beam vibration using a nonlinear spring for damage represantation", *J. Mech. Mater. Struct.*, **3**(8), 1589-1604.
Mokasji, P.S. and Mendelsohn, D.A. (2008), "Nonlinear vibration of an edge-cracked beam with a cohesive zone, 1: Nonlinear bending load-displacement relations for a linear softening cohesive law", *J. Mech. Mater. Struct.*, **3**(8), 1573-1588.
Peng, Z.K., Lang, Z. and Chu, F.L. (2008), "Numerical analysis of cracked beams using nonlinear output frequency responses functions", *Comput. Struct.*, **86**(17-18), 1809-1818.
Sundermeyer, J.N. and Weaver, R.L. (1995), "On crack identification and characterization in a beam by non-linear vibration analysis", *J. Sound Vib.*, **183**(5), 857-871.
Tada, H., Paris, P.C. and Irwin, G.R. (1985), *The Stress Analysis of Cracks Handbook*, Paris Production Incorporated and Del Research Corporation.
Yan, T., Yang, J. and Kitipornchai, S. (2012), "Nonlinear dynamics response of an edge-cracked functionally graded Timoshenko beam under parametric excitation", *Nonlin. Dyn.*, **67**(1), 527-540.
Younesian, D., Marjani, S.R. and Esmailzadeh, E. (2013), "Nonlinear vibration analysis of harmonically excites cracked beams on viscoelastic foundations", *Nonlin. Dyn.*, **71**(1-2), 109-120.
Wei, K.X., Ye, L., Ning, L.W. and Liu, Y.C. (2013), "Nonlinear dynamics response of a cracked beam under multi-frequency excitation", *Adv. Vib. Eng.*, **12**(5), 431-446.
Zienkiewichz, O.C. and Taylor, R.L. (2000), *The Finite Element Method*, Fifth Edition, Volume 2: Solid Mechanics, Butterworth-Heinemann, Oxford.

CC

Appendix

The components of the material stiffness matrix: the axial stiffness matrix $\mathbf{K}_M^a$, the bending stiffness matrix $\mathbf{K}_M^b$ and the shearing stiffness matrix $\mathbf{K}_M^s$ are as follows

$$\mathbf{K}_M^a = \frac{EA}{L_0}\begin{vmatrix} c_m^2 & c_m s_m & -c_m\gamma_m L_0/2 & -c_m^2 & -c_m s_m & -c_m\gamma_m L_0/2 \\ c_m s_m & s_m^2 & -\gamma_m L_0 s_m/2 & -c_m s_m & -s_m^2 & -\gamma_m L_0 s_m/2 \\ -c_m\gamma_m L_0/2 & -\gamma_m L_0 s_m/2 & \gamma_m^2 L_0^2/4 & c_m\gamma_m L_0/2 & \gamma_m L_0 s_m/2 & \gamma_m^2 L_0^2/4 \\ -c_m^2 & -c_m s_m & c_m\gamma_m L_0/2 & c_m^2 & c_m s_m & c_m\gamma_m L_0/2 \\ -c_m s_m & -s_m^2 & \gamma_m L_0 s_m/2 & c_m s_m & s_m^2 & \gamma_m L_0 s_m/2 \\ -c_m\gamma_m L_0/2 & -\gamma_m L_0 s_m/2 & \gamma_m^2 L_0^2/4 & c_m\gamma_m L_0/2 & \gamma_m L_0 s_m/2 & \gamma_m^2 L_0^2/4 \end{vmatrix} \tag{A1}$$

$$\mathbf{K}_M^b = \frac{EI_0}{L_0}\begin{vmatrix} 0 & 0 & 0 & 0 & 0 & 0 \\ 0 & 0 & 0 & 0 & 0 & 0 \\ 0 & 0 & 1 & 0 & 0 & -1 \\ 0 & 0 & 0 & 0 & 0 & 0 \\ 0 & 0 & 0 & 0 & 0 & 0 \\ 0 & 0 & -1 & 0 & 0 & 1 \end{vmatrix} \tag{A2}$$

$$\mathbf{K}_M^s = \frac{GA}{L_0}\begin{vmatrix} s_m^2 & -c_m s_m & -\alpha_1 L_0 s_m/2 & -s_m^2 & c_m s_m & -\alpha_1 L_0 s_m/2 \\ -c_m s_m & c_m^2 & c_m\alpha_1 L_0/2 & c_m s_m & -c_m^2 & c_m\alpha_1 L_0/2 \\ -\alpha_1 L_0 s_m/2 & c_m\alpha_1 L_m/2 & \alpha_1^2 L_0^2/4 & \alpha_1 L_0 s_m/2 & -c_m\alpha_1 L_0/2 & \alpha_1^2 L_0^2/4 \\ -s_m^2 & c_m s_m & \alpha_1 L_0 s_m/2 & s_m^2 & -c_m s_m & \alpha_1 L_0 s_m/2 \\ c_m s_m & -c_m^2 & -c_m\alpha_1 L_0/2 & -c_m s_m & c_m^2 & -c_m\alpha_1 L_0/2 \\ -\alpha_1 L_0 s_m/2 & c_m\alpha_1 L_0/2 & \alpha_1^2 L_0^2/4 & \alpha_1 L_0 s_m/2 & -c_m\alpha_1 L_0/2 & \alpha_1^2 L_0^2/4 \end{vmatrix} \tag{A3}$$

where m stands for beam midpoint, ξ=0, and ω_m =(θ_1+θ_2)/2, ω_m=θ_m+φ, c_m=cosω_m, s_m=sinω_m, e_m=Lcos(θ_m−ψ)/L_0−1, α_1=1+e_m and γ_m=Lsin(ψ−θ_m)L_0 (See Fig. A1 for symbols). The axis of the considered beam initially is taken as horizontal, therefore φ=0. The matrix **S** is defined as follows

$$\mathbf{S} = \begin{bmatrix} EA & 0 & 0 \\ 0 & GA & 0 \\ 0 & 0 & EI \end{bmatrix} \tag{A4}$$

$\mathbf{B}_m$ matrix is as follows

$$\mathbf{B}_m = B\big|_{\xi=0} = \frac{1}{L_0}\begin{bmatrix} -c_m & -s_m & -\frac{1}{2}L_0\gamma_m & c_m & s_m & -\frac{1}{2}L_0\gamma_m \\ s_m & -c_m & \frac{1}{2}L_0(1+e_m) & s_m & -c_m & \frac{1}{2}L_0(1+e_m) \\ 0 & 0 & -1 & 0 & 0 & 1 \end{bmatrix} \tag{A5}$$

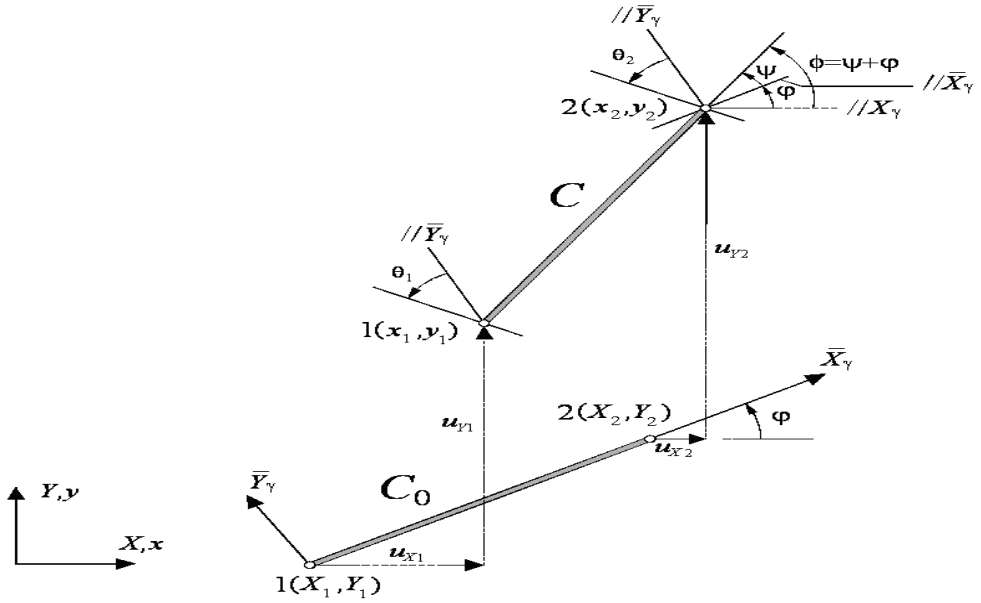

Fig. A1 Plane beam element with arbitrarily oriented reference configuration (Felippa 2013)

The geometric stiffness matrix K_G is given as follows

$$\mathbf{K}_G = \frac{N_m}{2}\begin{bmatrix} 0 & 0 & s_m & 0 & 0 & s_m \\ 0 & 0 & -c_m & 0 & 0 & -c_m \\ s_m & -c_m & -\frac{1}{2}L_0(1+e_m) & -s_m & c_m & -\frac{1}{2}L_0(1+e_m) \\ 0 & 0 & -s_m & 0 & 0 & -s_m \\ 0 & 0 & c_m & 0 & 0 & c_m \\ s_m & -c_m & -\frac{1}{2}L_0(1+e_m) & -s_m & c_m & -\frac{1}{2}L_0(1+e_m) \end{bmatrix}$$

$$+\frac{V_m}{2}\begin{bmatrix} 0 & 0 & c_m & 0 & 0 & c_m \\ 0 & 0 & s_m & 0 & 0 & s_m \\ c_m & s_m & -\frac{1}{2}L_0\gamma_m & -c_m & -s_m & -\frac{1}{2}L_0\gamma_m \\ 0 & 0 & -c_m & 0 & 0 & -c_m \\ 0 & 0 & -s_m & 0 & 0 & -s_m \\ c_m & s_m & -\frac{1}{2}L_0\gamma_m & -c_m & -s_m & -\frac{1}{2}L_0\gamma_m \end{bmatrix} \tag{A6}$$

in which N_m and V_m are the axial and shear forces which are evaluated at the midpoint. The internal nodal force vector is as follows Felippa (2013)

$$\mathbf{P}=L_0\mathbf{B}_m^T\mathbf{z}=\begin{bmatrix} -c_m & -s_m & \frac{1}{2}L_0\gamma_m & c_m & s_m & \frac{1}{2}L_0\gamma_m \\ s_m & -c_m & -\frac{1}{2}L_0(1+e_m) & s_m & -c_m & -\frac{1}{2}L_0(1+e_m) \\ 0 & 0 & -1 & 0 & 0 & 1 \end{bmatrix} \tag{A7}$$

where $\mathbf{z}^T=N\ V\ M$. The external nodal force vector can be expressed as follows

$$f=b\int_h\int_{L_0}\begin{bmatrix} 1-\xi_1 & 0 & 0 \\ 0 & 1-\xi_1 & 0 \\ 0 & 0 & 1-\xi_1 \\ 1-\xi_1 & 0 & 0 \\ 0 & 1-\xi_1 & 0 \\ 0 & 0 & 1-\xi_1 \end{bmatrix}\begin{bmatrix} f_X \\ f_Y \\ 0 \end{bmatrix}dX\ dY+b\int_{L_0}\begin{bmatrix} 1-\xi_1 & 0 & 0 \\ 0 & 1-\xi_1 & 0 \\ 0 & 0 & 1-\xi_1 \\ 1-\xi_1 & 0 & 0 \\ 0 & 1-\xi_1 & 0 \\ 0 & 0 & 1-\xi_1 \end{bmatrix} \tag{A8}$$

where f_X, f_Y are the body forces, t_X, t_Y, m_Z are the surface loads in the X, Y directions and about the Z axis.